Available online at www.eccomasproceedia.org
Eccomas Proceedia COMPDYN (2017) 4145-4160

ECCOMAS
Proceedia

COMPDYN 2017
6th ECCOMAS Thematic Conference on
Computational Methods in Structural Dynamics and Earthquake Engineering
M. Papadrakakis, M. Fragiadakis (eds.)
Rhodes Island, Greece, 15–17 June 2017

SEISMIC RELIABILITY-BASED DESIGN OF INELASTIC STRUCTURES WITH DIFFERENT VALUES OF THE POST-YIELDING STIFFNESS ISOLATED BY FPS

P. Castaldo[1], B. Palazzo[2], G. Alfano[2] and M. F. Palumbo[2]

[1]Department of Structural, Geotechnical and Building Engineering (DISEG), Politecnico di Torino,
Corso Duca degli Abruzzi, 24, Turin, Italy (corresponding author);
e-mail: paolo.castaldo@polito.it; pcastaldo@unisa.it

[2]Department of Civil Engineering, University of Salerno,
Via Giovanni Paolo II (SA), Italy;
e-mail: palazzo@unisa.it; gae.alfano@gmail.com; mfr.plm@gmail.com

Keywords: seismic isolation; friction coefficient; seismic reliability; ductility demand; behaviour factor; post-yield stiffness..

Abstract. *This work aims to evaluate the seismic reliability of nonlinear systems, considering both a hardening and softening post-yielding behavior, isolated by friction pendulum devices (FPS) for different values of the strength reduction factor. The isolated structure is described through an equivalent 2dof model, whereas, the FPS behavior is described by a velocity dependent model. An extensive parametric study is carried out encompassing a wide range of inelastic building properties considering different values of the post-yielding stiffness, different seismic intensity levels and considering the friction coefficient as a random variable. Defined a set of natural seismic records and scaled to the seismic intensity corresponding to life safety limit state for L'Aquila site (Italy) according to NTC08, the yielding characteristics of the superstructures are consequently designed according to NTC08 for different values of the strength reduction factor. Incremental dynamic analyses (IDA) are developed to evaluate the seismic fragility curves of both the inelastic superstructure and the isolation level assuming different values of the corresponding limit states. Integrating the fragility curves with the seismic hazard curves related to L'Aquila site (Italy), the reliability curves of the inelastic base-isolated structural systems, with a design life of 50 years, are derived and proposed in order to provide useful design recommendations depending on both the strength reduction factors and post-yielding behavior.*

Peer-review under responsibility of the organizing committee of COMPDYN 2017.
doi: 10.7712/120117.5712.16852

1 INTRODUCTION

Friction pendulum system (FPS) represents an effective technique for the seismic isolation [1] of building frames [2]-[3]. The modeling aspects of the FPS isolation technique (e.g., [4]-[7]) and the effects of the variation of both systems and FP devices as well the influence of the seismic input have been object of many works. Over the years, within the issue of the passive control of structures, many works have developed new design strategies and methodologies [8]-[14]. Reliability analysis and reliability-based optimization of base-isolated systems including uncertainties of both the isolation devices properties and ground motion characteristics have been evaluated by [15]-[18].

In [19], the life-cycle cost analysis of the abovementioned r.c. 3D system isolated by FPS bearings has been evaluated for increasing values of the isolation degree. The seismic reliability-based design (SRBD) approach for elastic systems has been proposed by Castaldo et al. [20]. Optimal friction coefficient values have been defined in [21] depending on the soil condition.

Seismic codes [22]-[26] aim to keeping the response of base-isolated structures, under strong earthquake events, elastic in order to avoid non linear amplification phenomenon [27] by means of low values of the strength reduction factor [22],[26] or behaviour factor [23]-[24]. In particular, the Italian seismic code, NTC08 [24], the European seismic code Eurocode 8 [23] and the Japanese building code [25] provide a maximum behavior factor value of 1.5 for base-isolated structures, without explicitly distinguishing the different terms (i.e., ductility and overstrength factors). The US seismic design codes, ASCE 7 [22], prescribes the strength reduction factor for a seismically isolated structure to be 0.375 times the one for a corresponding fixed-base structure and no larger than 2. Indeed, Vassiliou et al. [28], proved that if the base-isolated structures are designed to respond inelastically, the displacement ductility demand of the inelastic base-isolated structure is 3 times the strength reduction factor. Furthermore, [29] and [30] proved that the equal displacement rule and the equal energy rule cannot be used for isolated systems. Reliability-based relationship between the ductility-dependent strength reduction factors and the displacement ductility demand are proposed by [31] for a perfectly elastoplastic structural system equipped with FPS and located in L'Aquila site (Italy) for different structural system properties.

The aim of this work is to further advance the study of Castaldo et al. [31] evaluating the seismic reliability of non linear base-isolated systems with hardening and softening post-yield stiffness and for increasing strength reduction factors.

2 NON-LINEAR SOFTENING MODEL OF A BASE-ISOLATED STRUCTURE WITH FPS

The model used in this study is the 2dof system proposed by Kelly [35], modified to account for the non-linear responses of both the isolation level and the superstructure (Fig. 1). The bearing response is modelled using a bilinear hysteretic response envelope, a typical model used for FPS system in the hypothesis to consider the horizontal component of the FP displacements [2].Therefore, the bearing restoring force is:

$$f_b = \frac{W}{R} u_b + \mu_d W \operatorname{sgn}\left(\dot{u}_b\right) \tag{1}$$

where $W = \left(m_b + m_s\right)g$ is the weight on the bearing, g is the gravity constant, R is the radius of curvature of the FPS, u_b is the displacement of the isolation level with respect to the

ground, μ_d is the bearing friction coefficient, sgn is the signum function of the sliding velocity, $\dot{u}_b$.

The friction coefficient at sliding velocity $\dot{u}_b$, according to Mokha et el. and Constantinou et al. [4]-[6], can be approximated by the following equation:

$$\mu_d = f_{\max} - (f_{\max} - f_{\min})\exp(-\alpha \dot{u}_b) \tag{2}$$

where $f_{\max}$ and $f_{\min}$ are the friction coefficient attained at high and at very low velocities of sliding respectively, α is a constant for a given pressure, temperature and condition of FPS interfaces, assumed equal to 30 and the ratio $f_{\max} / f_{\min}$ equal to 3 [21],[31].

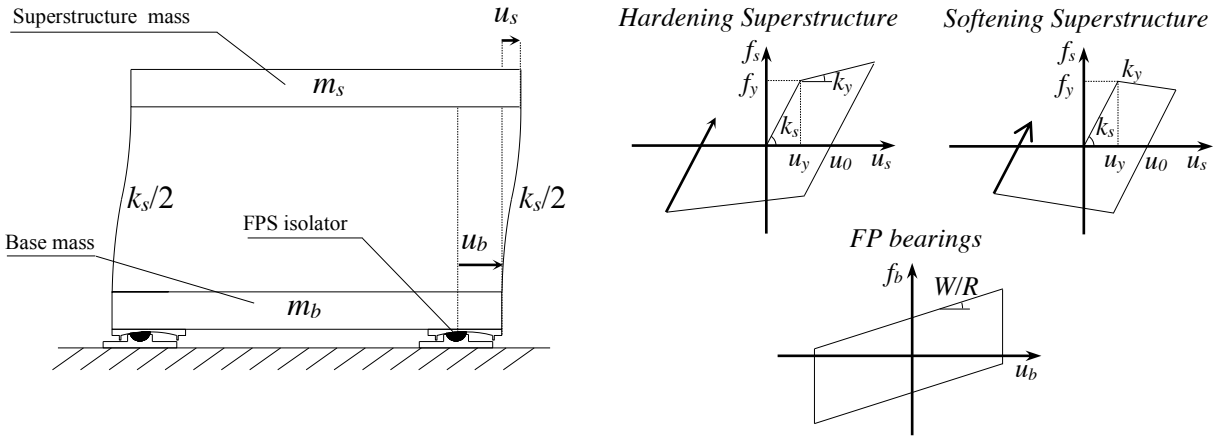

Figure 1: 2dof model of a building isolated with FPS.

Regarding the inelastic response of the superstructure, the behaviour is described using a non-linear constitutive law, for which the restoring force varies if the superstructure is in the elastic or in plastic phases. The superstructure is in the elastic phases if Eqn.(3) is satisfied and the corresponding restoring force is given by Eqn.(4).

$$\left|u_{s,i} - u_{0,i-1}\right| < y\left(u_{s,i}\right) \tag{3}$$

$$f_{s,i}\left(u_{s,i}\right) = k_s\left(u_{s,i} - u_{0,i-1}\right) \tag{4}$$

In the equations (3) and (4), $f_{s,i}$ is the superstructure restoring force at time instant i, $u_{s,i}$ is the deformation of the superstructure with respect to the base at time instant i, $u_{0,i-1}$ is the maximum plastic excursion at time instant $(i-1)$, k_s is the elastic stiffness of the superstructure. The function $y(u_{s,i})$ is the yielding condition that is not univocally defined because the elastic domain translates, so the yielding limits are different in function of the direction of the displacement. The yielding condition can assume the following values:

$$y(u_{s,i}) = u_y + S\left(u_{s,i} - u_y\right) \text{ for } (u_{0,i-1} \geq 0 \ \& \ u_{s,i} > u_{0,i-1}) \text{ and } (u_{0,i-1} < 0 \ \& \ u_{s,i} < u_{0,i-1})$$

$$y(u_{s,i}) = u_y - S\left(u_{s,i} - u_y\right) \text{ for } (u_{0,i-1} \leq 0 \ \& \ u_{s,i} > u_{0,i-1}) \text{ and } (u_{0,i-1} > 0 \ \& \ u_{s,i} < u_{0,i-1}) \tag{5a,b}$$

where u_y is the yield displacement, whose yield force is f_y, S is the ratio between the post-yield and the elastic stiffness [36],[37]:

$$S = \frac{k_y}{k_s} \tag{6}$$

The superstructure is in the plastic phases if:

$$\left|u_{s,i}-u_{0,i-1}\right| \geq y(u_{s,i}) \tag{7}$$

the restoring force applies:

$$f_{s,i}\left(u_s\right)=k_s(u_{s,i}-y)\,\mathrm{sgn}(u_{s,i}-u_{0,i-1}) \tag{8}$$

It follows that the response of an inelastic 2dof system isolated with FPS devices (Fig. 1) to the seismic input $\ddot{u}_g\left(t\right)$ is governed by Eqn. (9):

$$\begin{aligned}&\left(m_b+m_s\right)\ddot{u}_b+m_s\ddot{u}_s+c_b\dot{u}_b+\frac{W}{R}u_b+\mu_d W\,\mathrm{sgn}\,\dot{u}_b=-\left(m_b+m_s\right)\ddot{u}_g\\&m_s\ddot{u}_b+m_s\ddot{u}_s+c_s\dot{u}_s+f_s\left(u_s\right)=-m_s\ddot{u}_g\end{aligned} \tag{9a,b}$$

where m_s and m_b are respectively the mass of the superstructure and of the basement, c_s is the superstructure viscous damping constant, c_b is the bearing viscous damping constant. By introducing the mass ratio $\gamma=\dfrac{m_s}{\left(m_s+m_b\right)}$ [35], the isolation $\omega_b=\sqrt{\dfrac{k_b}{\left(m_s+m_b\right)}}=\sqrt{\dfrac{g}{R}}$ and structural $\omega_s=\sqrt{k_s/m_s}$ circular frequency, the isolation $\xi_b=c_b/2\left(m_b+m_s\right)\omega_b$ and structural $\xi_s=c_s/2m_s\omega_s$ damping ratio, and dividing Eqn.(9a) by m_b+m_s and Eqn.(9b) by m_s, the equations of motion can be reduced to a non-dimensional form:

$$\begin{aligned}&\ddot{u}_b+\gamma\ddot{u}_s+2\xi_b\omega_b\dot{u}_b+\frac{g}{R}u_b+\mu_d g\,\mathrm{sgn}\,\dot{u}_b=-\ddot{u}_g\\&\ddot{u}_b+\ddot{u}_s+2\xi_s\omega_s\dot{u}_s+a_s\left(u_s\right)=-\ddot{u}_g\end{aligned} \tag{10a,b}$$

where $a_s\left(u_s\right)=f_s\left(u_s\right)/m_s$ is the dimensionless force of the superstructure that changes if the superstructure is in an elastic or plastic phase. The seismic isolation degree [40] is an indicator of isolation system efficiency for elastic structures and results to be the ratio between the isolation $T_b=2\pi/\omega_b$ and structural $T_s=2\pi/\omega_s$ period of vibration: $I_d=T_b/T_s$ [40].

2.1 Behavior factor and displacement ductility of the non-linear superstructure

Regarding the inelastic response of a superstructure ([40]), characterized by a single degree of freedom with an hardening or softening behavior the strength reduction factor is defined as:

$$q=\frac{f_{s,el}}{f_y}=\frac{u_{s,el}}{u_y} \tag{11}$$

where $f_{s,el}$ and $u_{s,el}$ are, respectively, the minimum yield strength and yield deformation required for the superstructure to remain elastic during a ground motion, or the peak response values for the corresponding linear system. Note that in the case of softening systems, assumed as the equivalent model representative of multistory frame taking count of the $P-\Delta$ effect [38],[39] the abovementioned behaviour factor q represents only the ductility-dependent term strength reduction factor because overstrength capacities, assumed with the equivalent model, are completely absent. Therefore, the reduction factor or behavior factor, hereinafter denoted as q, is consistent with the code provisions [22]-[26] in the case of a unitary overstrength factor and with the one discussed by [31] for the case of softening systems.

The displacement ductility, μ, of the superstructure is defined as:

$$\mu=\frac{u_{\mathrm{s,max}}}{u_y} \tag{12}$$

where $u_{s,\max} = \left|u_s(t)\right|_{\max}$ is the peak displacement of the inelastic system

3 UNCERTAINTIES WITHIN THE SEISMIC RELIABILITY OF NON-LINEAR SUPERSTRUCTURES EQUIPPED WITH FPS

According to the structural performance (SP) evaluation method [41]-[43], the seismic reliability assessment of buildings is based on the coupling between SP levels [44] and associated exceeding probabilities during its design life [45]-[46]. Coherently with the PEER-like modular approach [47] and performance-based earthquake engineering (PBEE) approach [48]-[49], the uncertainties related to the seismic input intensity are separated from those related to the characteristics of the record (record-to-record variability) by introducing an intensity measure (*IM*). The approach, as also discussed in [20],[31], is based on calculating the convolution integral between the fragility curves and a seismic hazard curve, expressed in terms of the same *IM*, related to a reference site, in order to define the mean annual rates exceeding the limit states and, next, using a Poisson distribution, evaluate the exceeding probabilities in the time frame of interest (e.g., 50 years). Superstructure properties are not included as random variables as discussed in [31],[50]. Regarding the uncertainty of the sliding friction coefficient at large velocity of the FP devices, an appropriate Gaussian probability density function (PDF) is employed and the Latin Hypercube Sampling (LHS) method [31]-[34] is adopted as random sampling technique in order to define the input data set, as also described in [31] in order to compare the results. In particular, the friction coefficient at large velocity is modelled through a Gaussian probability density function (PDF), defined from 0.5% to 5.5% with a mean value equal to 3% [51] and a standard deviation equal to the dispersion of a corresponding uniform PDF truncated on both sides to 0.5% and 5.5%. As widely discussed in [31], 15 values of the random variable $f_{\max}$ are sampled through the LHS method.

3.1 Seismic input and intensity measure (IM) description

In this study, the spectral displacement, $S_D(\xi_b, T_b)$, at the isolated period of the system, $T_b = 2\pi/\omega_b$ and for the damping ratio ξ_b, is assumed as intensity measure. The spectral displacement is related to the spectral acceleration $S_D(\xi_b, T_b) = S_{pa}(\xi_b, T_b)/\omega_b^2$. In the analyses carried out in this study, the damping ratio ξ_b is taken equal to zero, consistently with other works which assume that friction is the only source of damping in the isolators [31],[52]. The corresponding *IM* is hereinafter denoted as $S_D(T_b)$ and it is assumed ranging from 0 m to 0.45 m according to the seismic hazard of L'Aquila site (Italy) [24]. A set of 30 natural ground motion records, selected within the ground motion databases [53]-[55]. The details and characteristics of the selected ground motion records may be found in [31].

4 PARAMETRIC STUDY: INCREMENTAL DINAMIC ANALYSIS RESULT

The first step to determinate the seismic reliability of the inelastic softening base-isolated equivalent systems, located in L'Aquila site (Italy), consists in developing incremental dynamic analyses (IDAs) [56]. An extensive parametric study is carried out encompassing a wide range of the parameter combinations related to isolation level and superstructure, according to Eqn.(10).

4.1 Parametric study

The parametric study encompasses several values related to elastic and inelastic building properties combined with the 15 input values of the friction coefficient random variable, the 30 ground motion records scaled to the different levels of the $IM = S_D(T_b)$, ranging from 0 m to 0.45 m. The deterministic parameters are: the seismic isolation degree I_d equal to 4, the isolation period of vibration T_b equal to 6 s, the mass ratio γ assumed equal to 0.6 and 0.8, the behavior factor q ranging from 1.1 to 2 according to the codes [22]-[25] and the post-yield stiffness S assumed equal to ± 0.03 [36]-[39]. It follows that several equivalent 2dof structural systems, with isolation damping ratio ξ_b and superstructure damping ratio ξ_s respectively equal to 0% and 2%, are defined. In order to develop the incremental non-linear dynamic analyses, the yielding characteristics of each equivalent structural system have to be designed. Therefore, the elastic equivalent 2dof system with a design friction coefficient equal to 3% has been subjected to the set of 30 seismic records, scaled to the $IM = S_D(T_b)$ value related to the life safety limit state (NTC08 [24]) for L'Aquila site (Italy): the $IM = S_D(T_b)$ is equal to 0.26 m for T_b =6 s [31]. The dynamic analyses, carried out in Matlab-Simulink [68], of the 32 base-isolated systems equipped with velocity-dependent FPS and with a superstructure linear behaviour have allowed to evaluate the average values of both the yield strength $f_{y,\text{average}}$ and displacement $u_{y,\text{average}}$ of the superstructure for each value of q, according to Eqn.(13) and as developed in [31]. In this way, all the yielding characteristics of the seveal equivalent non-linear structural systems have been defined according to the codes [22]-[25] in order to compare the results with the outcomes described in [31] and evaluate the influence of the post-yield stiffness.

$$u_{y,average} = \frac{f_{y,average}}{k_s} = \frac{f_{s,el,average}}{k_s q} = \frac{u_{s,el,average}}{q} \tag{11}$$

4.2 Incremental dynamic analysis (IDA) result for different structural parameters

The above-mentioned equivalent non-linear structural systems, with the different structural parameters (q and S) and combined for each value of the sampled friction coefficient, are subjected to the 30 ground motions, scaled to the several intensity levels values within the IDA. The isolated non-linear systems are modelled in Matlab-Simulink [68] to solve the coupled equations (Eqn.(10)) and determine the isolation and superstructure responses. In particular, the Runge-Kutta-Fehlberg integration algorithm available in Matlab-Simulink has been employed. A total number of 450 simulations has been carried out for each IM and parameters combination. Note that for a structure with a softening behaviour the maximum available ductility capacity, assumed herein as the collapse condition, is reached when the reduction in the strength is complete. This assumption represents the failure condition assumed within the numerical analyses. The results of the incremental non-linear dynamic analyses (IDAs), taking into account the collapsed systems, have allowed to estimate the superstructure and isolation response parameters, expressed in terms of displacement ductility demand μ and of maximum displacement of the isolation level with respect to the ground $u_{b,\max} = |u_b(t)|_{\max}$, respectively, adopted as the engineering demand parameters (EDPs) and assumed to follow a lognormal distribution [21],[31],[48],[52]. Knowing the sample lognormal mean $\mu_{\ln}(EDP)$ and the dispersion $\beta(EDP)$, it is possible to determine the 50$^{\text{th}}$, 84$^{\text{th}}$ and 16$^{\text{th}}$ percentile of

each lognormal distribution [20]. The IDA results of the isolation level and the superstructure are respectively illustrated in Fig.s 2-3 depending on the intensity measure *IM* and on the behavior factor q.

Note that the 50th, 84th and 16th percentiles, related to both isolation level and superstructure shown in the figures of this section, have been evaluated only from the results without considering the failures. The presence of the data characterized by the dynamic collapses has been taken into account within the seismic fragility assessment as discussed later. This means that, for the case of softening systems, some results from the IDA curves do not represent the real response of these systems. In particular, all IDA curves, related to softening systems, illustrate that for quite all parameter combinations and *IM* levels, the number of dynamic collapses is very high.

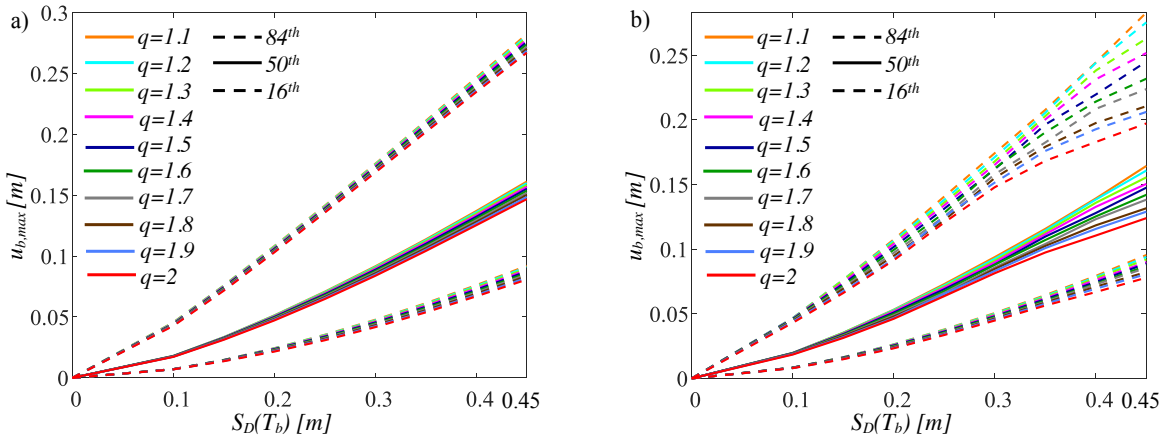

Fig. 2. IDA curves of the isolation level with γ =0.6, I_d=4, and T_b=6 s for S=+0.03 (a), S=-0.03 (b)

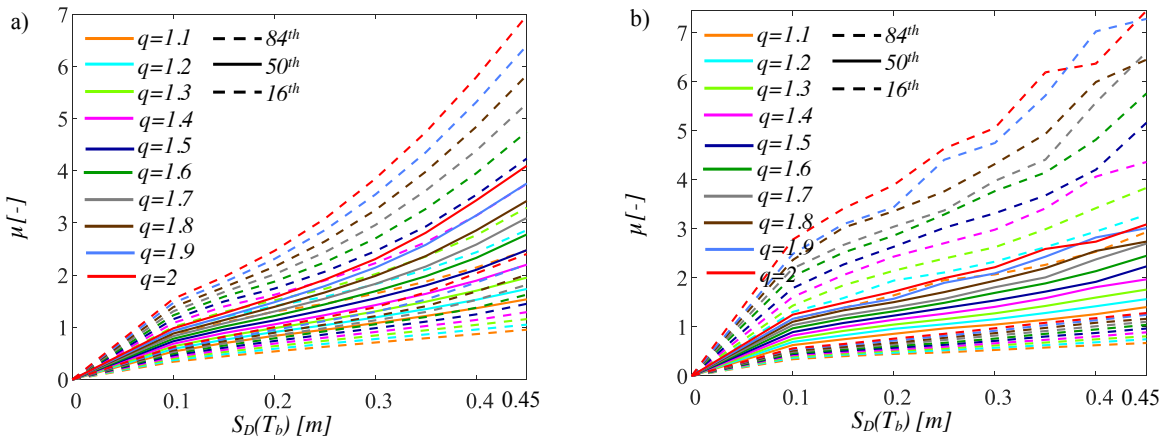

Fig. 3. IDA curves of the superstructure with γ =0.6, I_d=4, and T_b=6 s for S=+0.03 (a), S=-0.03 (b).

Fig. 2 shows the IDA results regarding the isolation level response parameter $u_{b,\max}$, whereas Fig. 3 shows the IDA curves regarding the superstructure EDP μ. The statistics of the EDP μ are strongly influenced by q: the increase of the strength reduction factor q leads to a very high increase of the displacement ductility demand μ.

5 SEISMIC FRAGILITY OF INELASTIC SOFTENING STRUCTURES WITH FPS

In order to evaluate the seismic fragility, defined as the probabilities P_f exceeding different limit states (*LSs*) at each level of the *IM*, of the isolation level and of the superstructure, the limit state *LS* thresholds have to be defined. In particular, the performance levels of the isolation system are assumed in terms of radius in plan of the concave surface, r [m]; while, the performance levels of the superstructure are defined in terms of available displacement ductility, μ [-]. Tables 1-2 show the *LS* for the isolation level and the superstructure related to the collapse and the safety limit state respectively considering structural systems in ordinary conditions and neglecting aging effects [57]-[67]. For both collapse and life safety *LSs*, characterized by appropriate failure probabilities in 50 years [19],[42],[43], several thresholds are analyzed because the scope of the study is to define the *LS* thresholds to be employed for a reliable design or verification of base-isolated non linear systems analyzing the response of the equivalent inelastic 2dof model, as discussed in the following sections.

	$LS_{b,1}$	$LS_{b,2}$	$LS_{b,3}$	$LS_{b,4}$	$LS_{b,5}$	$LS_{b,6}$	$LS_{b,7}$	$LS_{b,8}$	$LS_{b,9}$	$LS_{b,10}$
r [m]	*0.05*	*0.1*	*0.15*	*0.2*	*0.25*	*0.3*	*0.35*	*0.4*	*0.45*	*0.5*
$p_f(50\ years)=1.5\cdot10^{-3}$										

Table 1: Limit state thresholds for the isolation level.

	$LS_{\mu,1}$	$LS_{\mu,2}$	$LS_{\mu,3}$	$LS_{\mu,4}$	$LS_{\mu,5}$	$LS_{\mu,6}$	$LS_{\mu,7}$	$LS_{\mu,8}$	$LS_{\mu,9}$	$LS_{\mu,10}$
μ [-]	*1*	*2*	*3*	*4*	*5*	*6*	*7*	*8*	*9*	*10*
$p_f(50\ years)=2.2\cdot10^{-2}$										

Table 2: Limit state thresholds for the superstructure.

The probabilities P_f exceeding different *LSs* at each level of the *IM*, are numerically computed for each combination of the structural properties (1280 equivalent structural systems) and then fitted through lognormal distributions [20]. In this phase, as for the softening systems and with the aim to consider both the collapse and not-collapse cases for each parameter combination at each *IM* level, the total probability theorem allows to estimate the probability exceeding a limit state at each intensity measure level considering the collapse number [69] as follows:

$$P_{SL}(IM = im) = (1 - F_{EDP|IM=im}(LS_{EDP})) \cdot \frac{N_{not-collapse}}{N} + 1 \cdot \left(1 - \frac{N_{not-collapse}}{N}\right) \qquad (12)$$

where N is the total number of analyses for the structural system at each *IM* level, and $N_{not-collapse}$ is the number of numerical simulations without any collapse. The first term of Eq.(12) defines the probability exceeding a *LS* corresponding to not-collapsing structural models [69]. The fragility curves are plotted in Fig.s 4-7 showing the exceedance probabilities P_f versus the ground motion intensity. Each figure contains several curves corresponding to the different values of the mass ratio and strength reduction factors q considered. Only the results corresponding to some limit state thresholds and to I_d=4 and T_b=6 s are reported because of space constraints.

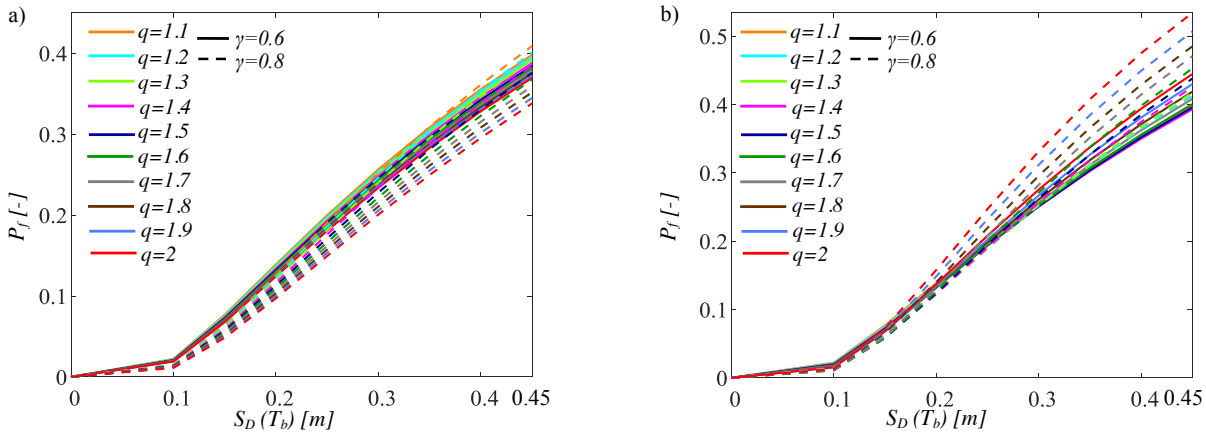

Fig. 4. Seismic fragility curves of the isolation level related to $LS_{b,4}$=0.2 m, for I_d=4 and T_b=6 s, S=+0.03 (a), I_d=4 and T_b=6 s, S=-0.03 (b).

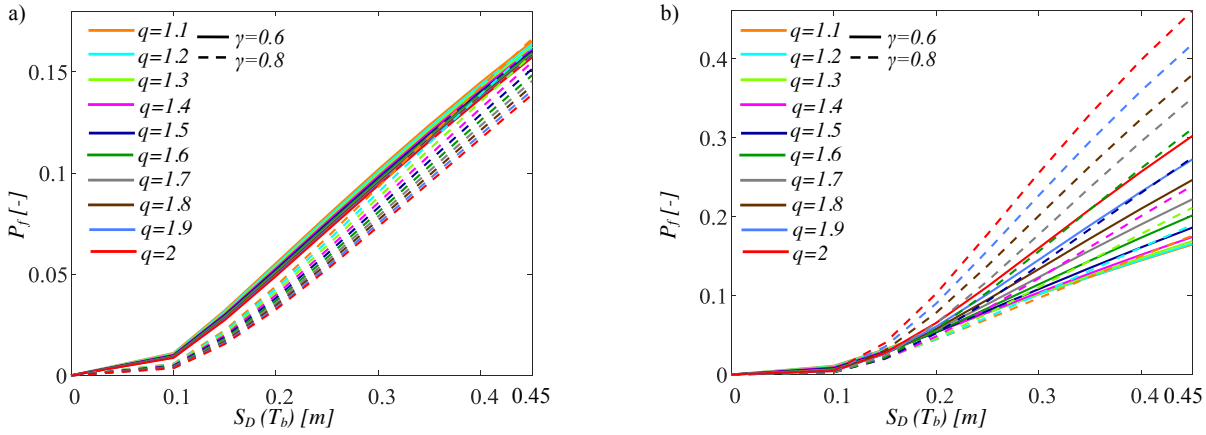

Fig. 5. Seismic fragility curves of the isolation level related to $LS_{b,8}$=0.4 m, for I_d=4 and T_b=6 s, S=+0.03 (a), I_d=4 and T_b=6 s, S=-0.03 (b).

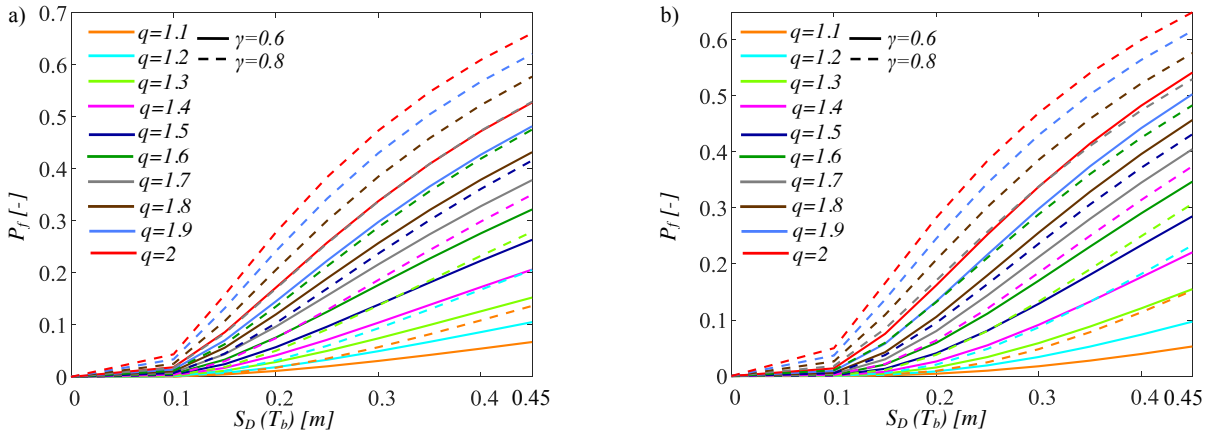

Fig. 6. Seismic fragility curves of the superstructure related to $LS_{\mu,3}$=3, for I_d=4 and T_b=6 s, S=+0.03 (a), I_d=4 and T_b=6 s, S=-0.03 (b).

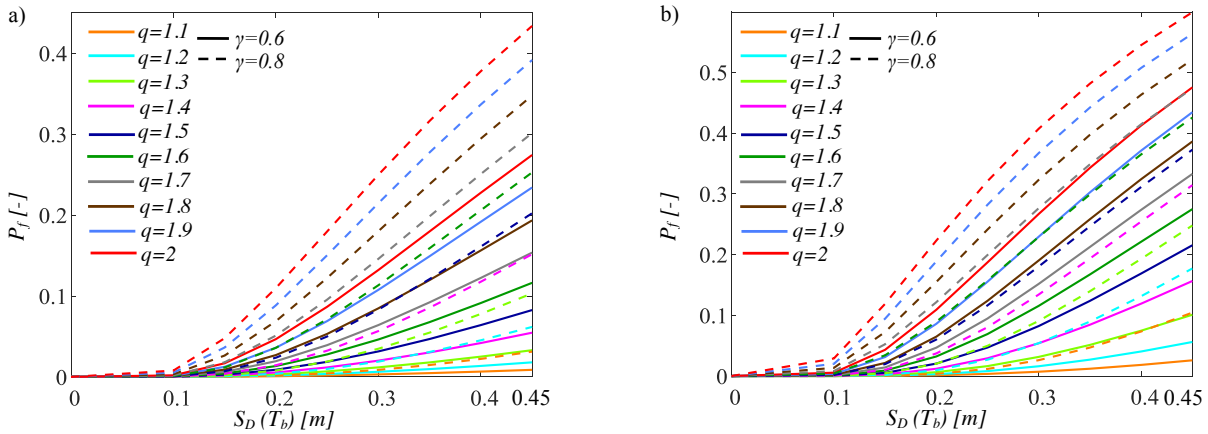

Fig. 7. Seismic fragility curves of the superstructure related to $LS_{\mu,5}$=5, for I_d=4 and T_b=6 s, S=+0.03 (a), I_d=4 and T_b=6 s, S=-0.03 (b).

Fig.s 4-5 show the fragility curves regarding the isolation level. Generally, the seismic fragility decreases for increasing the limit state thresholds. For all limit states, the exceeding probabilities slightly decrease for higher values of γ. The influence of γ is amplified also due to the uncertainty of the friction coefficient. Especially, in the case of high values of limit state thresholds, the exceeding probabilities P_f increase by increasing q. Furthermore, a decrease of the post-yield stiffness ratio S also leads to higher probability of exceedance.

Fig.s 6-7 show the fragility curves regarding the superstructure. Similarly to the isolation seismic fragility curves, the exceeding probabilities decrease by increasing the limit state thresholds. Higher values of γ lead to slightly higher values of the exceeding probabilities as well as higher values of q lead to strongly higher values of seismic fragility. Moreover, the post-yield stiffness ratio S strongly influences leading to a higher displacement ductility demand for lower values of S.

6 SEISMIC RELIABILITY OF INELASTIC BASE-ISOLATED STRUCTURES WITH FPS

Integrating the previously defined seismic fragility curves with the seismic hazard curves, expressed in terms of the same IM, $S_D(T_b)$, related to the reference site (L'Aquila (Italy)), allows to calculate the mean annual rates exceeding the limit states in the time frame of interest. These latter ones have to be transformed into exceeding probabilities in the time frame of interest (e.g., 50 years) by using a Poisson distribution in order to evaluate the seismic reliability of the non-linear structures isolated by FPS. In this work, the local seismic hazard of L'Aquila site (Italy), soil class B, with geographic coordinates 42°38'49''N and 13°42'25''E, has been considered according to [31]. The seismic hazard curves have been defined in terms of $IM = S_D(T_b)$ and related to the isolated period analysed in the parametric study, according to NTC08 [24]. The seismic hazard curve represents the average values of the annual rate exceeding the $IM = S_D(T_b)$ level, as widely discussed in [31].

The linear regression curves, for the isolation level, defined in the range between 10^{-1}-10^{-4} in the semi-logarithmic space, representative of the seismic reliability of the friction devices, are plotted for different displacement thresholds, varying from 0.05 m to 1 m, in Fig. 8. The lowest value of R-square is higher than to 0.8 confirming a quite good effectiveness of the regressions. It is possible to observe that the seismic reliability of the isolation level is slightly influenced by γ as previously described for the fragility curves. The increase of the strength

reduction factor leads a decrease of the seismic reliability. These performance curves, ($SP_{isolator}$), (Fig. 8), can be used for the preliminary design of the dimensions in plan of the FP devices, depending on the elastic and inelastic structural properties in an area with a seismic hazard similar to that considered, in order to respect the expected reliability level. In particular, an exceeding probability of P_f = 1.5·10-3 (related to the collapse limit state, reliability index β=3 in 50 years) [42]-[45] can be respected through a radius in plan r having a dimension lower than 1m, in the case of very low values of the behaviour factor.

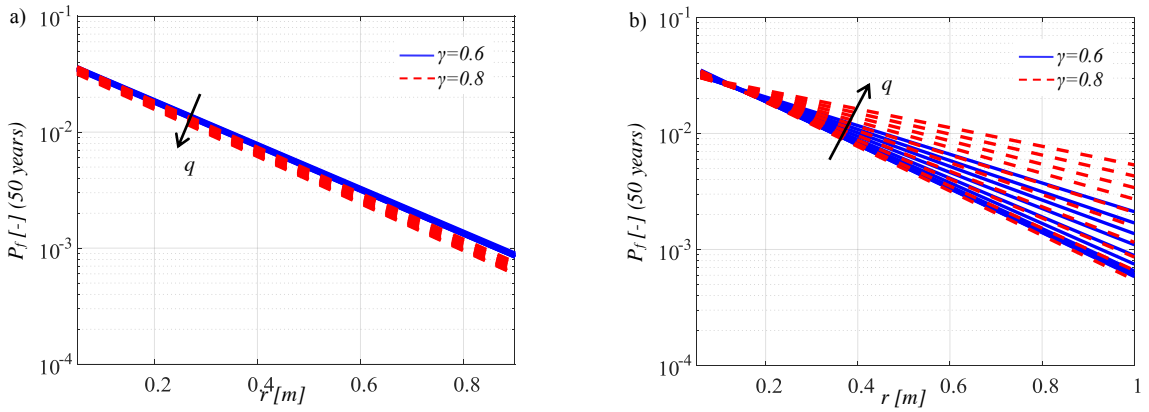

Fig. 8. Seismic reliability curves of the isolation level related to I_d=4, for T_b=6 s, S=+0.03 (a), T_b=6 s, S=-0.03 (b). The arrow denotes the increasing direction of q.

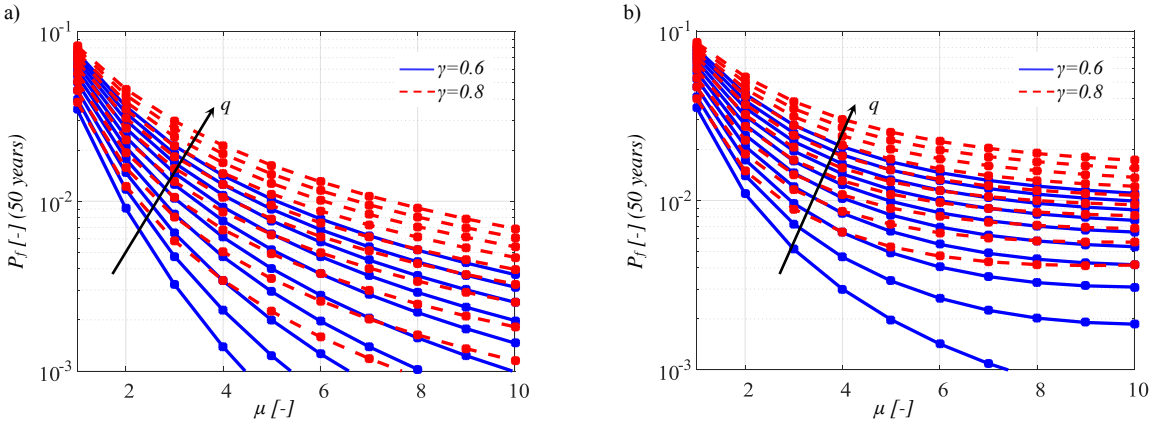

Fig. 9. Seismic reliability curves of the superstructure related to I_d=4, for T_b=6 s, S=+0.03 (a), T_b=6 s, S=-0.03 (b). The arrow denotes the increasing direction of q.

In Fig. 9, the results, evaluated for $\mu \geq 1$, representing the seismic reliability (SP curves) of the inelastic superstructure, that is, the exceeding probabilities (Complementary CDFs) in the time frame of interest (50 years), are plotted in logarithmic scale for the different *LS* thresholds in terms of the displacement ductility and for different values of the superstructure properties. The seismic reliability of the superstructure decreases for higher values of γ, q and decreasing values of S (from hardening to softening systems).

7 CONCLUSIONS

This paper describes the seismic reliability of inelastic softening structural systems, equipped with friction pendulum isolators (FPS) through an extensive parametric study encompassing a wide range of elastic and inelastic building properties, different seismic intensity levels and considering the friction coefficient and the uncertainties related to the seismic

input intensity and to the characteristics of the records as random variables within the uncertainties relevant to the problem. The isolated system is described by a 2dof system in order to take account of the hardening and softening superstructure response, and the FPS behavior is described by employing a velocity dependent model. Considering a set of seismic records, the inelastic characteristics of the structural systems are designed according to the life safety limit state for L'Aquila site (Italy), as provided by NTC08 provisions, for increasing strength reduction factors. Then, incremental dynamic analyses are developed to evaluate the response statistics related to both superstructure and isolation level for different structural properties, strength reduction factors and post-yield hardening and softening stiffness ratios. The estimates of the response statistics, then, are used for deriving seismic fragility curves for the superstructure and the isolation level assuming different values of the corresponding limit state thresholds. In the final part of the work, considering the seismic hazard curves related to L'Aquila site (Italy), as provided by NTC08 provisions, regarding systems isolated by FP bearings with a design life of 50 years, seismic reliability-based design (SRBD) abacuses are proposed with the aim to design the radius in plan of the FP isolators, highlighting the effects of the post-yield hardening and softening stiffness. In particular, an exceeding probability related to the collapse limit state can be achieved through a radius in plan r having a dimension lower than 1m, in the case of very low values of the behaviour factor for softening systems.

As for the superstructure, the seismic reliability assessment demonstrates the negative effects due to the post-yield softening stiffness able to strongly amplify the displacement ductility demand for isolated structure designed to yield under the expected seismic base shear and may lead to collapse. The proposed SRBD formulae can be used for the preliminary design of hardening structures and verification of base-isolated hardening or softening regular frames, located in an area characterized by a seismic hazard similar to that considered.

8 REFERENCES

[1] Christopoulos C, Filiatrault A. *Principles of Passive Supplemental Damping and Seismic Isolation*. IUSS Press: Pavia, Italy, 2006.

[2] Zayas VA, Low SS, Mahin SA. A simple pendulum technique for achieving seismic isolation. *Earthquake Spectra* 1990; 6:317–33.

[3] Su L, Ahmadi G, Tadjbakhsh IG. Comparative study of base isolation systems. *Journal of Engineering Mechanic* 1989; 115:1976–92.

[4] Mokha A, Constantinou MC, Reinhorn AM. Teflon Bearings in Base Isolation. I: Testing. *J. Struct. Eng*. 1990; 116(2): 438-454.

[5] Constantinou MC, Mokha A, Reinhorn AM. Teflon Bearings in Base Isolation. II: Modeling. *J. Struct. Eng*. 1990; 116(2):455-474.

[6] Constantinou MC, Whittaker AS, Kalpakidis Y, Fenz DM, Warn GP. Performance of Seismic Isolation Hardware Under Service and Seismic Loading. Technical Report, 2007.

[7] Almazàn JL, De la Llera JC. Physical model for dynamic analysis of structures with FPS isolators. *Earthquake Engineering and Structural Dynamics* 2003; 32:1157–1184.

[8] Palazzo B., Castaldo P., Marino I., The Dissipative Column: A New Hysteretic Damper," Buildings 5(1), 163-178, 2015, doi:10.3390/buildings5010163.

[9] Castaldo P., Integrated Seismic Design of Structure and Control Systems. Springer International Publishing: New York, 2014 . DOI 10.1007/978-3-319-02615-2.

[10] De Iuliis M., Castaldo P., An energy-based approach to the seismic control of one-way asymmetrical structural systems using semi-active devices, Ingegneria Sismica - Inter-

national Journal of Earthquake Engineering XXIX(4):31-42, 2012.

[11] M.T. Giugliano, A. Longo, R. Montuori, V.Piluso, Influence of homoschedasticity hypothesis of structural response parameters on seismic reliability of CB-frames, *Georisk*, **5**(2), 120-131, 2011.

[12] M.T. Giugliano, A. Longo, R. Montuori, V. Piluso, Seismic reliability of traditional and innovative concentrically braced frames, *Earthquake Engineering and Structural Dynamics*, **40**(13), 1455–1474, 2011.

[13] A. Longo, R. Montuori, V. Piluso, Seismic reliability of V-braced frames: Influence of design methodologies, *Earthquake Engineering and Structural Dynamics*, **38**(14), 1587–1608, 2009.

[14] Ayyub BM, McCuen RH. Probability, statistics, and reliability for engineers. 2nd ed. NY: CRC Press; 2002.

[15] Chen J, Liu W, Peng Y, Li J. Stochastic seismic response and reliability analysis of base-isolated structures. *J Earthquake Eng* 2007;11:903‑24.

[16] Alhan C, Gavin HP. Reliability of base isolation for the protection of critical equipment from earthquake hazards. *Eng Struct* 2005;27:1435‑49.

[17] Zou XK, Wang Q, Li G, Chan CM. Integrated reliability-based seismic drift design optimization of base-isolated concrete buildings. *J Struct Eng* 2010;136:1282‑95.

[18] Mishra SK, Roy BK, Chakraborty S. Reliability-based-design-optimization of base isolated buildings considering stochastic system parameters subjected to random earthquakes. *Int J Mech Sci* 2013;75:123‑33.

[19] Castaldo P., Palazzo B., Della Vecchia P., (2016) "Life-cycle cost and seismic reliability analysis of 3D systems equipped with FPS for different isolation degrees", Engineering Structures, 125;349–363, http://dx.doi.org/10.1016/j.engstruct.2016.06.056.

[20] Castaldo P., Amendola G., Palazzo B., (2017) "Seismic fragility and reliability of structures isolated by friction pendulum devices: Seismic reliability-based design (SRBD)", Earthquake Engineering and Structural Dynamics, 46(3); 425–446, DOI: 10.1002/eqe.2798.

[21] Castaldo P., Ripani M., "Optimal design of friction pendulum system properties for isolated structures considering different soil conditions", Soil Dynamics and Earthquake Engineering, 2016, 90:74–87, DOI: 10.1016/j.soildyn.2016.08.025.

[22] Structural Engineering Institute. Minimum design loads for buildings and other structures (Vol. 7, No. 5). Amer Society of Civil Engineers, 2010.

[23] European Committee for Standardization. Eurocode 8-Design of Structures for Earthquake Resistance. Part 1: General Rules, Seismic Actions and Rules for Buildings, Brussels, 2004.

[24] NTC08. Norme tecniche per le costruzioni. Gazzetta Ufficiale del 04.02.08, DM 14.01.08, Ministero delle Infrastrutture.

[25] Japanese Ministry of Land, Infrastructure and Transport, Notification No. 2009–2000, Technical Standard for Structural Specifications and Calculation of Seismically Isolated Buildings 2000.

[26] Quantification of Building Seismic Performance Factors, FEMA P695 / June 2009.

[27] Occhiuzzi, A, Veneziano, D.and Van Dyck, J. (1994) Seismic design of base isolated structures, Savidis (Ed.), Balkema, Rotterdam, NL.

[28] Vassiliou M.F., Tsiavos A., Stojadinović B. Dynamics of inelastic base-isolated structures subjected to analytical pulse ground motions. *Eart. Eng. and Str. Dyn.* 2013; 42:2043–2060.

[29] Newmark NM, Hall WJ. Seismic design criteria for nuclear reactor facilities, Report 46, Building Practices for Disaster Mitigation, National Bureau of Standards, 1973.

[30] Miranda E, Bertero VV. Evaluation of strength reduction factors for earthquake-resistant design. Earthquake Spectra 1994; 10:357–379.

[31] Castaldo P., Palazzo B. and Ferrentino T. Seismic reliability-based ductility demand evaluation for inelastic base-isolated structures with friction pendulum devices, Earthquake Engineering and Structural Dynamics 2017; 46:1245–1266, DOI: 10.1002/eqe.2854.

[32] Mckey MD, Conover WJ, Beckman RJ. A comparison of three methods for selecting values of input variables in the analysis from a computer code. Technometrics 1979;21:239-45.

[33] Vořechovský M, Novák D. Correlation control in small-sample Monte Carlo type simulations I: a simulated annealing approach. *Probabilistic Engineering Mechanics* 2009;24(3):452‑62.

[34] Celarec D, Dolšek M. The impact of modelling uncertainties on the seismic performance assessment of reinforced concrete frame buildings. *Engineering Structures* 2013;52:340‑354.

[35] Naeim F, Kelly JM. Design of Seismic Isolated Structures: From Theory to Practice. John Wiley & Sons, Inc.; 1999.

[36] Hatzigeorgiou GD. Ductility demand spectra for multiple near- and far-fault earthquakes. *Soil Dynamics and Earthquake Engineering* 2010;30 170-183.

[37] Hatzigeorgiou GD, Papagiannopoulos GA, Beskos DE. Evaluation of maximum seismic displacements of SDOF systems form their residual deformation. *Engineering Structures* 2011;33 3422-3431.

[38] Gupta A, Krawinkler H. Seismic demands for performance evaluation of steel moment resisting frame structures. The John A. Blume Earth. Eng. Center report No. 132, June 1999.

[39] Adam C, Ibarra LF, Krawinkler H. Evaluation of P-Delta effects in non-deteriorating MDOF structures from equivalent SDOF systems. *13th Word Conference on Earthquake Engineering*, Vancouver, B.C., Canada 2004, Paper No. 3407.

[40] Palazzo B. Seismic Behavior of base-isolated Buildings. Proc. International Meeting on earthquake Protection of Buildings, Ancona, 1991.

[41] Collins KR, Stojadinovic B. Limit states for performance-based design. 12WCEE, 2000.

[42] Bertero RD, Bertero VV. Performance-based seismic engineering: the need for a reliable conceptual comprehensive approach. *Earthquake Engineering and Structural Dynamics* 2002;31:627–652 (DOI: 10.1002/eqe.146).

[43] Aoki Y, Ohashi Y, Fujitani H, Saito T, Kanda J, Emoto T, Kohno M. Target seismic performance levels in structural design for buildings. 12WCEE, 2000.

[44] SEAOC Vision 2000 Committee. Performance-based seismic engineering. Report prepared by Structural Engineers Association of California, Sacramento, CA., 1995.

[45] CEN – European Committee for Standardization. Eurocode 0: Basis of Structural De-

sign. Final draft. Brussels, 2006.

[46] Saito T, Kanda J, Kani N. Seismic reliability estimate of building structures designed according to the current Japanese design code. Proc.s of the Str. Eng.s World Congress, 1998.

[47] Cornell CA, Krawinkler H. Progress and challenges in seismic performance assessment. PEER Center News 2000;4(1):1-3

[48] Aslani H, Miranda E. Probability-based seismic response analysis. *Engineering Structures* 2005; **27**(8): 1151-1163.

[49] Porter KA. An overview of PEER's performance-based earthquake engineering methodology. Proceedings, *Proceedings of the 9th International Conference on Application of Statistics and Probability in Civil Engineering* (*ICASP9*), San Francisco, California, 2003; 973-980.

[50] Kulkarni JA, Jangid RS. Effects of superstructure flexibility on the response of base-isolated structures. Shock and Vibration 2003;26:1-13.

[51] http://www.fipindustriale.it/

[52] Ryan KL, Chopra AK (2004). Estimation of Seismic Demands on Isolators Based on Nonlinear Analysis. J. Struct. Eng., 130(3), 392–402.

[53] PEER, *Pacific Earthquake Engineering Research Center* http://peer.berkeley.edu/

[54] ITACA, *Italian Accelerometric Archive* http://itaca.mi.ingv.it/ItacaNet/itaca10_links.htm

[55] ISESD, *Internet-Site for European Strong-Motion Data* http://www.isesd.hi.is/ESD_Local/frameset.htm

[56] Vamvatsikos D, Cornell CA. Incremental dynamic analysis. *Earthquake Engineering and Structural Dynamics* 2002; 31(3): 491–514.

[57] Palazzo, B., Castaldo, P., Mariniello, A. Time-variant structural reliability of R.C. structures affected by chloride-induced deterioration, American Concrete Institute, ACI Special Publication 2015-January (SP 305), pp. 19.1-19.10.

[58] Faleschini F., Hofer L., Zanini M.A., Dalla Benetta M., Pellegrino C. Experimental behavior of beam-column joints made with EAF concrete under cyclic loading. Engineering Structures 139, 81-95, 2017.

[59] Faleschini F., Zanini M.A., Pellegrino C., Pasinato S. Sustainable management and supply of natural and recycled aggregates in a medium-size integrated plant. Waste Management 49, 146-155, 2016.

[60] Etse, G.J., Ripani, M., Vrech, S.M. "Fracture energy-based thermodynamically consistent gradient model for concrete under high temperature," Proceedings of the 8th International Conference on Fracture Mechanics of Concrete and Concrete Structures, FraMCoS 2013, 1506-1515.

[61] Etse, G., Ripani, M., Caggiano, A. & Schicchi, D.S. "Strength and durability of concrete subjected to high temperature: continuous and discrete constitutive approaches," American Concrete Institute, ACI Special Publication 2015-January (SP 305), 9.1-9.18.

[62] Etse, G., Ripani, M. & Mroginski, J.L. "Computational failure analysis of concrete under high temperature," Computational Modelling of Concrete Structures - Proceedings of EURO-C 2014, 2:715-722.

[63] Etse, G., Vrech, S.M. & Ripani, M. "Constitutive theory for Recycled Aggregate Concretes subjected to high temperature," Construction and Building Materials; 111: 43-53,

2016.

[64] Mroginski, J.L., Etse, G., Ripani, M. "A non-isothermal consolidation model for gradient-based poroplasticity," PANACM 2015 - 1st Pan-American Congress on Computational Mechanics, in conjunction with the 11th Argentine Congress on Computational Mechanics, MECOM 2015, pp. 75-88.

[65] Ripani, M., Etse, G., Vrech, S. & Mroginski, J.L. "Thermodynamic gradient-based poroplastic theory for concrete under high temperature," International Journal of Plasticity; 61: 157-177, 2014.

[66] Ripani, M., Etse, G., Vrech, S. "Recycled aggregate concrete: localized failure assessment in thermodynamically consistent non-local plasticity framework", Computers and Structures, 178: 47–57, 2017, doi: 10.1016/j.compstruc.2016.08.007.

[67] Vrech, S.M., Ripani, M. & Etse, G. "Localized versus diffused failure modes in concrete subjected to high temperature," PANACM 2015 - 1st Pan-American Congress on Computational Mechanics, in conjunction with the 11th Argentine Congress on Computational Mechanics, MECOM 2015, pp. 225-236.

[68] Math Works Inc. MATLAB-High Performance Numeric Computation and Visualization Software. User's Guide. Natick: MA, USA, 1997.

[69] Bazzurro P, Cornell CA, Shome N, Carballo JE (1998): Three proposals for characterizing MDOF nonlinear seismic response. Journal of Structural Engineering, 124(11), 1281-1289.

[70] Peter Fajfar, M.EERI. A Nonlinear Analysis Method for Performance Based Seismic Design. Earthquake Spectra, Vol.16, No.3, pp.573-592, August 2000.

[71] Paulay T., Priestley M. J. N.: Seismic design of reinforced concrete and masonry buildings, John Wiley & Sons, 1992.